

## Ultrafast Bidirectional Photoswitching of a Spiropyran

Johannes Buback,<sup>†</sup> Martin Kullmann,<sup>†</sup> Florian Langhoyer,<sup>†</sup> Patrick Nuernberger,<sup>†</sup>  
Ralf Schmidt,<sup>‡</sup> Frank Würthner,<sup>‡</sup> and Tobias Brixner<sup>\*†</sup>

*Institut für Physikalische und Theoretische Chemie and Institut für Organische Chemie,  
Universität Würzburg, Am Hubland, 97074 Würzburg, Germany*

Received July 15, 2010; E-mail: brixner@phys-chemie.uni-wuerzburg.de

**Abstract:** We report on bidirectional photochemical switching of 6,8-dinitro-1',3',3'-trimethylspiro[2H-1-benzopyran-2,2'-indoline] (6,8-dinitro-BIPS) between the ring-closed spiropyran and the ring-open merocyanine form. This is studied by femtosecond three-color pump–repump–probe experiments. Both ring opening and ring closure are photoinduced. Completion of an entire cycle, consisting of opening and subsequent closure, can be achieved within 40 ps. A much shorter time (<6 ps) is needed for the converse cycle, consisting of initial ring closure and subsequent ring opening. Furthermore, we perform pump–probe experiments with ultraviolet/visible pump and visible/mid-infrared probe pulses for an unambiguous spectroscopic identification of the open and closed molecular forms. Following visible excitation of the ring-open molecules, ultrafast ring closure is observed directly in the mid-infrared. The quantum efficiencies for ring opening and ring closure starting from the respective equilibrium states are determined to be approximately 9% and 40%. These results show that 6,8-dinitro-BIPS is an ultrafast bidirectional molecular switch exhibiting a high quantum efficiency.

### Introduction

Photochromic systems are defined by a controllable light-induced change of color. They have a vast variety of applications, from sunglasses to data storage.<sup>1–3</sup> Among the molecular switches, those with a reversible ring closure have drawn much attention due to well-separated absorption bands of the two isomers. Since the usability of photochromic molecular switches depends further on the switching time scales and the respective quantum yields for both directions, for an optimization of molecular switches it is essential to understand the participating photoreactions on a molecular level. Therefore, ultrafast studies have been performed, e.g., on dithienylethene derivatives,<sup>4,5</sup> fulgides and fulgimides,<sup>6,7</sup> and spiropyrans.<sup>8–14</sup> Table 1 shows quantum yields for dithienylethenes, fulgides, and fulgimides.

The quantum yields of the ring-closing and ring-opening reactions can be chemically tuned. Either ring closure can be achieved with very high quantum yield at the cost of the quantum efficiency of ring opening, or vice versa. Typically though, the achievable molecular quantum yield is higher for ring closure than for ring opening (Table 1). Also, in some cases the reaction rates are slow due to triplet-state pathways. However, for switching applications, good quantum yields and high speed are desired for switching in both directions. For spiropyrans, only photochemical

**Table 1.** Comparison of Quantum Efficiencies of Exemplary Molecular Switches Based on a 6 $\pi$ -Electrocyclic Reaction

derivative of	quantum efficiency, %	
	ring closure (trans $\rightarrow$ cis) <sup>e</sup>	ring opening (cis $\rightarrow$ trans) <sup>e</sup>
dithienylethene <sup>15,a</sup>	50	<2
dithienylethene <sup>15,b</sup>	86	0.15
indolylfulgimide <sup>16,c</sup>	28	14
furylfulgide <sup>17</sup>	20	12
azobenzene <sup>18</sup>	25	50
6,8-dinitro-BIPS <sup>d</sup>	40	9

<sup>a</sup> Bis(2,4-dimethyl-5-phenylthiophen-3-yl)perfluorocyclopentene substituted with benzonitrile: 50% not capable of ring closure. <sup>b</sup> Polymer of bis(2,4-dimethyl-5-phenylthiophen-3-yl)perfluorocyclopentene: isomer not capable of ring closure suppressed in polymer. <sup>c</sup> Isomer not capable of ring closure: < 3% <sup>d</sup> Result of this work, see Discussion. <sup>e</sup> Quantum efficiencies refer to trans/cis isomerization for the case of azobenzene and to ring closure/opening for all other examples.

ring opening has been directly demonstrated so far.<sup>8,9,13,14</sup> In this work, we show that a suitable spiropyran system can be switched photochemically in both directions with competitive quantum yields on an ultrafast time scale.

The ring-closed form of a spiropyran (Figure 1, left structure) consists of a pyran and an indoline moiety with orthogonal orientation. Thus, both moieties are independent<sup>19</sup> and absorb in the ultraviolet only. Ring opening completely changes the

<sup>†</sup> Institut für Physikalische und Theoretische Chemie.

<sup>‡</sup> Institut für Organische Chemie.

(1) Dürr, H.; Bouas-Laurent, H. *Photochromism: Molecules and Systems*; Elsevier: Amsterdam, 2003.

(2) Feringa, B. L. *Molecular Switches*; Wiley-VCH Verlag GmbH: Weinheim, 2001.

(3) Bouas-Laurent, H.; Dürr, H. *Pure Appl. Chem.* **2001**, *73*, 639–665.

(4) Ern, J.; Bens, A. T.; Martin, H.; Kuldova, K.; Trommsdorff, H. P.; Kryschi, C. *J. Phys. Chem. A* **2002**, *106*, 1654–1660.

(5) Murakami, M.; Miyasaka, H.; Okada, T.; Kobatake, S.; Irie, M. *J. Am. Chem. Soc.* **2004**, *126*, 14764–14772.

(6) Heinz, B.; Malkmus, S.; Laimgruber, S.; Dietrich, S.; Schulz, C.; Rück-Braun, K.; Braun, M.; Zinth, W.; Gilch, P. *J. Am. Chem. Soc.* **2007**, *129*, 8577–8584.

(7) Draxler, S.; Brust, T.; Malkmus, S.; DiGirolamo, J. A.; Lees, W. J.; Zinth, W.; Braun, M. *Phys. Chem. Chem. Phys.* **2009**, *11*, 5019–5027.

(8) Rini, M.; Holm, A.; Nibbering, E. T. J.; Fidler, H. *J. Am. Chem. Soc.* **2003**, *125*, 3028–3034.

(9) Ern, J.; Bens, A. T.; Martin, H.; Kuldova, K.; Trommsdorff, H. P.; Kryschi, C. *J. Phys. Chem. A* **2002**, *106*, 1654–1660.

(10) Wohl, C. J.; Kuciauskas, D. *J. Phys. Chem. B* **2005**, *109*, 22186–22191.

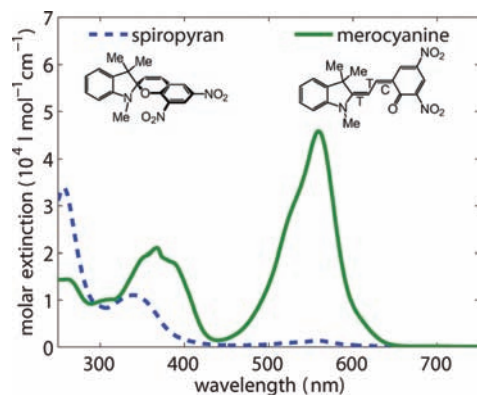


**Figure 1.** Spiropyran and merocyanine main isomers (TTC, describing the configuration around the three central double bonds) of 6,8-dinitro-BIPS and their corresponding steady-state absorption spectra in chloroform. The ring-closed spiropyran can be opened with light from the ultraviolet spectral region, whereas the merocyanine can be closed with light from either the ultraviolet or the visible spectral region. The spiropyran spectrum was obtained after almost complete merocyanine bleaching in the spectrometer.

molecule's electronic and structural properties. In the ring-open form (merocyanine, Figure 1, right structure), the two chromophores are positioned such that one large planar  $\pi$ -system emerges, leading to a strong absorption in the visible spectral region.<sup>20</sup> Hence, the angle between the chromophores is the relevant switching reaction coordinate. The electronic changes due to switching make spiropyran potential candidates for optical memories,<sup>21</sup> whereas the structural changes could be used as a switch of molecular or even biological properties, enhancing or stopping processes.<sup>22–24</sup>

The photochemical and thermal ring opening of several spiropyran has been investigated on the second to femtosecond time scale. It has been shown that, for unsubstituted spiropyran (1',3',3'-trimethylspiro[2H-1-benzopyran-2,2'-indoline] = BIPS), the photoinduced reaction is fast (28 ps) but inefficient.<sup>8,9,25</sup> The efficiency is strongly enhanced if a nitro group is substituted in the 6-position of the pyran moiety (6-nitro-BIPS). However, for such a substituted compound, the reaction time scale increases to nanoseconds due to a triplet pathway.<sup>13,26–28</sup>

Furthermore, although sketched in most spiropyran reaction schemes in the literature, there is no direct proof that the completely relaxed ring-open form can be switched back photochemically at all.<sup>10</sup> Only for the substituted compound with a second nitro group in the 8-position (6,8-dinitro-BIPS) has it been shown that irradiation with 400 nm light leads to a bleach of the visible absorption band on the picosecond time scale. This indirectly indicates formation of the ring-closed form.<sup>12</sup>

In this work, we present the first direct evidence for photochemical switching of a spiropyran in both directions. We investigate the bisubstituted 6,8-dinitro-BIPS and perform pump–probe transient absorption experiments in the ultraviolet, visible, and mid-infrared spectral regions. This combination of measurements allows a direct observation of the product formation. We then carry out three-pulse pump–repump–probe experiments, a scheme used to modify the course of a photo-induced reaction for additional insight,<sup>7,29–32</sup> demonstrating the complete open–closed–open as well as closed–open–closed photocycle. The organization of the manuscript is as follows: In the Experimental Section, we introduce our transient absorption setups and illustrate how the three-color pump–repump–probe data are obtained. Steady-state measurements and two-color pump–probe experiments on the ring-closing and the ring-opening reactions are presented first in the Results section. Those results represent a basis for understanding the three-color pump–repump–probe data in the ultrafast switching subsection at the end of the section. The insights obtained on the photochemical ring-closing and ring-opening reactions are then discussed and compared to results on related systems from the literature. Finally, a summary of the photochemistry of the spiropyran–merocyanine system is given.

## Experimental Section

6,8-Dinitro-BIPS was synthesized via the Knoevenagel condensation reaction of commercially available 1,2,3,3-tetramethyl-3H-indolium and 3,5-dinitrosalicylaldehyde, resulting in the merocyanine form of 6,8-dinitro-BIPS in 79% yield according to the literature<sup>1</sup> and characterized by HPLC, 400 MHz NMR spectroscopy, and high-resolution mass spectrometry (see Experimental Details below).

Steady-state absorption spectra were recorded in a 2 mm Suprasil cuvette with a Hitachi U-2000 spectrophotometer. Merocyanine spectra were recorded directly after the crystals were dissolved in chloroform.

The femtosecond laser system used for these experiments consists of a home-built Ti:sapphire oscillator and a home-built regenerative amplifier that generates pulses centered at 800 nm at a repetition rate of 1 kHz with a duration of 80 fs full width at half-maximum (fwhm). The visible (VIS) pump pulses were generated in a home-built non-collinear optical parametric amplifier (NOPA), resulting in 2  $\mu$ J pulses with about 50 fs fwhm duration tunable across the VIS spectral range. The 800 nm light was also used to generate 400 and 267 nm pump pulses using second-harmonic and sum-frequency generation in nonlinear crystals. The energy of the 400 nm pulses was reduced to 12  $\mu$ J in the mid-infrared (MIR) experiments, and the energy of the collinearly created 267 nm pulses was reduced to 1  $\mu$ J. The VIS and

- (11) Fidler, H.; Rini, M.; Nibbering, E. T. J. *J. Am. Chem. Soc.* **2004**, *126*, 3789–3794.
- (12) Hogley, J.; Pfeifer-Fukumura, U.; Bletz, M.; Asahi, T.; Masuhara, H.; Fukumura, H. *J. Phys. Chem. A* **2002**, *106*, 2265–2270.
- (13) Holm, A.; Rini, M.; Nibbering, E. T. J.; Fidler, H. *Chem. Phys. Lett.* **2003**, *376*, 214–219.
- (14) Holm, A.; Mohammed, O. F.; Rini, M.; Mukhtar, E.; Nibbering, E. T. J.; Fidler, H. *J. Phys. Chem. A* **2005**, *109*, 8962–8968.
- (15) Irie, M. *Chem. Rev.* **2000**, *100*, 1685–1716.
- (16) Wolak, M. A.; Thomas, C. J.; Gillespie, N. B.; Birge, R. R.; Lees, W. J. *J. Org. Chem.* **2003**, *68*, 319–326.
- (17) Siewertsen, R.; Renth, F.; Temps, F.; Sonnichsen, F. *Phys. Chem. Chem. Phys.* **2009**, *11*, 5952–5961.
- (18) Satzger, H.; Root, C.; Braun, M. *J. Phys. Chem. A* **2004**, *108*, 6265–6271.
- (19) Tyer, N. W.; Becker, R. S. *J. Am. Chem. Soc.* **1970**, *92*, 1289–1294.
- (20) Heiligman-Rim, R.; Hirshberg, Y.; Fischer, E. *J. Phys. Chem.* **1962**, *66*, 2465–2470.
- (21) Jiang, G.; Song, Y.; Guo, X.; Zhang, D.; Zhu, D. *Adv. Mater.* **2008**, *20*, 2888–2898.
- (22) Würthner, F.; Rebek, J. *Angew. Chem.* **1995**, *107*, 503–505.
- (23) Peters, M. V.; Stoll, R. S.; Kühn, A.; Hecht, S. *Angew. Chem., Int. Ed.* **2008**, *47*, 5968–5972.
- (24) Al-Atar, U.; Fernandes, R.; Johnsen, B.; Baillie, D.; Branda, N. R. *J. Am. Chem. Soc.* **2009**, *131*, 15966–15967.
- (25) Aramaki, S.; Atkinson, G. H. *J. Am. Chem. Soc.* **1992**, *114*, 438–444.
- (26) Yuzawa, T.; Shimojima, A.; Takahashi, H. *J. Mol. Struct.* **1995**, *352–353*, 497–507.
- (27) Görner, H. *Phys. Chem. Chem. Phys.* **2001**, *3*, 416–423.

- (28) Chibisov, A. K.; Görner, H. *Phys. Chem. Chem. Phys.* **2001**, *3*, 424–431.
- (29) Logunov, S. L.; Volkov, V. V.; Braun, M.; El-Sayed, M. A. *Proc. Natl. Acad. Sci. U.S.A.* **2001**, *98*, 8475–8479.
- (30) Farmanara, P.; Ritze, H.; Stert, V.; Radloff, W.; Hertel, I. V. *Eur. Phys. J. D* **2002**, *19*, 193–209.
- (31) Zamyatin, A. V.; Gusev, A. V.; Rodgers, M. A. J. *J. Am. Chem. Soc.* **2004**, *126*, 15934–15935.
- (32) Wohlleben, W.; Buckup, T.; Herek, J. L.; Motzkus, M. *ChemPhysChem* **2005**, *6*, 850–857.

the ultraviolet (UV) pump pulses can be delayed independently by  $\sim 3.7$  ns via two motorized delay stages.

We have used different sources for the probe pulse in order to cover wavelength regions from the MIR to the VIS spectral regime. The MIR probe was generated in a home-built optical parametric amplifier described elsewhere.<sup>33,34</sup> For probing in the VIS spectral region, a small fraction of the residual 800 nm pump light leaving the NOPA was focused in a linearly moving CaF<sub>2</sub> disk, generating a white-light continuum from 390 to 750 nm.<sup>35</sup> Colored filter glass (Schott BG 40) was used to cut off the 800 nm pump light before the sample. The probe light was spectrally dispersed by a spectrograph (Acton SP2500i) and digitized by a charge-coupled device (CCD) chip (Princeton Instruments Pixis 2K). By reading out the CCD chip in a special way, high frame rates of 1 kHz were achieved, making shot-to-shot measurements with the CCD chip possible and a separate reference beam unnecessary. The wavelength resolution of the VIS probe setup is  $\Delta\lambda = 1.4$  nm, and the temporal resolution is better than 50 fs.

For the pump–probe experiments, pump and probe pulses were focused individually and non-collinearly overlapped spatially in a 200  $\mu\text{m}$  flow cell. In the experiments with a VIS probe, the pump diameter in the focus was 40  $\mu\text{m}$ , and the probe beam diameter was 15–30  $\mu\text{m}$  (depending on the wavelength). In the MIR probe experiments, the probe beam was substantially larger, with a diameter of 400  $\mu\text{m}$ , and therefore the pump pulse's diameter was increased to 450  $\mu\text{m}$ . The angle between the linear polarizations of pump and probe pulses was set to the magic angle (54.7°) by turning the pump polarization with achromatic waveplates. For the experiments with 267 nm pump pulses, the solution in the reservoir was perpetually irradiated with an array of green light-emitting diodes (LEDs) to shift the equilibrium to the spiropyran form.

For the pump–repump–probe experiments, the solution was also converted to the spiropyran form with green LEDs. Pump and repump pulses were polarized orthogonal to each other. In order to isolate the dynamics induced by the pump–repump combination from the single-pump dynamics, two optical choppers with 90° phase difference were employed to block two consecutive pulses and let the next two pass. Since this was done for both pump pulses, this procedure gives rise to four pump–pulse combinations and corresponding transmitted probe light intensities:

1. VIS pump ( $I_{\text{VIS}}$ )
2. VIS pump and UV pump ( $I_{\text{UV+VIS}}$ )
3. UV pump ( $I_{\text{UV}}$ )
4. no pump ( $I_{\text{no pump}}$ )

Here, the transmitted probe intensities for a certain pump–probe combination are denoted with  $I$  and the respective subscript. From this we obtain three transient absorption signals (optical density changes,  $\Delta\text{OD}$ ):

$$\begin{aligned} 1. \quad \Delta\text{OD}_{\text{VIS}} &= -\lg \frac{I_{\text{VIS}}}{I_{\text{no pump}}} \\ 2. \quad \Delta\text{OD}_{\text{UV}} &= -\lg \frac{I_{\text{UV}}}{I_{\text{no pump}}} \\ 3. \quad \Delta\text{OD}_{\text{UV+VIS}} &= -\lg \frac{I_{\text{UV+VIS}}}{I_{\text{no pump}}} \end{aligned}$$

Recording all three combinations of transient absorption signals, the cooperative absorption signal due to interactions with both pump pulses ( $\Delta\text{OD}_{2p}$ ) is obtained via

$$\Delta\text{OD}_{2p} = \Delta\text{OD}_{\text{UV+VIS}} - \Delta\text{OD}_{\text{UV}} - \Delta\text{OD}_{\text{VIS}} \quad (1)$$

- (33) Hamm, P.; Kaindl, R. A.; Stenger, J. *Opt. Lett.* **2000**, *25*, 1798–1800.  
 (34) Wolpert, D.; Schade, M.; Brixner, T. *J. Chem. Phys.* **2008**, *129*, 094504.  
 (35) Nagura, C.; Suda, A.; Kawano, H.; Obara, M.; Midorikawa, K. *Appl. Opt.* **2002**, *41*, 3735–3742.

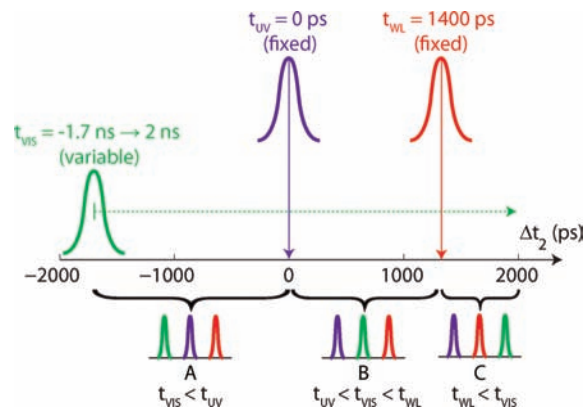


**Figure 2.** Scheme of the pump–repump–probe experiments. Whereas the UV pump (purple) and the VIS probe beam (red) remain at fixed positions ( $t_{\text{UV}}$  and  $t_{\text{WL}}$ , respectively), the delay of the VIS pump (green) ( $t_{\text{VIS}}$ ) is varied as indicated by the dashed green arrow. This results in the three different delay regions with different pulse sequences (A, B, and C) shown at the bottom.

Figure 2 illustrates the scanning scheme used in the pump–repump–probe experiments. The green pulse in this scheme represents the VIS pump pulse that induces ring closure of present merocyanine. The purple pulse represents the UV pump pulse that mostly induces ring opening of spiropyran since almost no merocyanine is present due to the constant illumination with the LED array. The red pulse represents the white-light (WL) probe pulse. UV and WL are both fixed in time and were set to 0 and 1400 ps, respectively, on the time delay axis  $\Delta t_2$ .

For investigating both switching directions, the VIS pulse is scanned from before the UV pulse to after the WL pulse ( $\Delta t_2 = -1.7$  ns  $\rightarrow \Delta t_2 = +2$  ns). Thus, the VIS pulse coincides with the UV pulse at  $\Delta t_2 = 0$  ps and with the WL pulse at  $\Delta t_2 = 1400$  ps. This gives rise to three delay regions, A, B, and C, with the different pulse sequences given at the bottom of Figure 2.

**Experimental Details:** (Z)-2,4-Dinitro-6-[(E)-2-(1,3,3-trimethyl-1,3-dihydroindol-2-ylidene)ethylidene]cyclohexa-2,4-dienone (**1**). 1,2,3,3-Tetramethyl-3*H*-indolium iodide (4.27 g, 14.2 mmol) was dissolved in dry EtOH (150 mL) under an argon atmosphere. Piperidine was added at 40 °C, and the solution was refluxed for 15 min. 3,5-Dinitrosalicylaldehyde (3.00 g, 14.2 mmol) in dry EtOH (150 mL) was added at room temperature, and the resulting mixture was refluxed for 3 h. The solvent was removed under reduced pressure, and the crude product was purified by column chromatography using silica and CH<sub>2</sub>Cl<sub>2</sub>/MeOH = 50:1 vol % as eluent. Precipitation from CH<sub>2</sub>Cl<sub>2</sub>/hexane and subsequent recrystallization from EtOH afforded pure **1** as a greenish red crystalline powder (4.12 g, 11.2 mmol, 79%). Purity of the compound >99% was verified by HPLC (normal phase, CHCl<sub>3</sub>/hexane 85:15). Mp: 262–265 °C (decomp). <sup>1</sup>H NMR (400 MHz, CDCl<sub>3</sub>):  $\delta$  8.52 (1 H, d, <sup>4</sup>*J* = 2.7 Hz, ArH), 8.11 (1 H, d, <sup>4</sup>*J* = 2.8 Hz, ArH), 7.13 (1 H, td, <sup>3</sup>*J* = 7.8 Hz, <sup>4</sup>*J* = 1.3 Hz, ArH), 7.03 (1 H, d, <sup>3</sup>*J* = 7.8 Hz, ArH), 6.96 (1 H, d, <sup>3</sup>*J* = 10.6 Hz, CH<sub>methine</sub>), 6.83 (1 H, td, <sup>3</sup>*J* = 7.4 Hz, <sup>4</sup>*J* = 1.0 Hz, ArH), 6.52 (1 H, d, <sup>3</sup>*J* = 7.2 Hz, ArH), 5.97 (1 H, d, <sup>3</sup>*J* = 10.5 Hz, CH<sub>methine</sub>), 2.69 (3 H, s, CH<sub>3</sub>), 1.28 (3 H, s, CH<sub>3</sub>), 1.13 (3 H, s, CH<sub>3</sub>). HRMS (ESI, positive mode, CH<sub>3</sub>CN/CHCl<sub>3</sub> = 1:1 vol %): calcd, *m/z* C<sub>19</sub>H<sub>18</sub>N<sub>3</sub>O<sub>5</sub>, 368.12410; found, 368.12410 ([M + H]<sup>+</sup>).

## Results

**Steady-State Spectra.** The ring-open merocyanine form and the ring-closed spiropyran form of 6,8-dinitro-BIPS differ strongly in their absorption spectra (Figure 1). In contrast to the majority of spiropyran–merocyanine systems,<sup>3</sup> including the unsubstituted and the 6-nitro-substituted variants, the predominant form in thermodynamic equilibrium of 6,8-dinitro-BIPS is the merocyanine, possessing a strong absorption in the

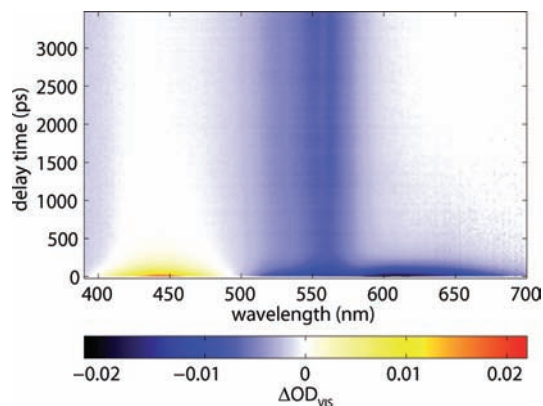


**Figure 3.** Spectrally resolved transient absorption data covering the visible spectral range, recorded with 560 nm pump pulses. The blue regions denote decreased absorption, thus revealing a permanent bleach at 560 nm and stimulated emission at 630 nm, whereas at 445 nm excited-state absorption (yellow-red) dominates the spectrum.

VIS range (540–610 nm). In chloroform the absorption band (Figure 1) is slightly red-shifted ( $\lambda_{\text{max}} = 559$  nm) in comparison to that in more polar solvents,<sup>12</sup> which suggests a prevalence of a zwitterionic ground state.<sup>36</sup> Upon irradiation with green light, the deeply purple merocyanine solution fades quickly. The absorption spectrum of the formed (ring-closed) spiropyran shown in Figure 1 exhibits two maxima ( $\lambda = 340$  nm and  $\lambda = 260$  nm). The thermal ring opening occurs on a time scale of minutes. After the spiropyran solution is illuminated with UV light (267 nm), the solution turns colored again due to merocyanine formation. Only slightly more than 50% of the initial merocyanine concentration can be recovered in the photostationary equilibrium because the formed merocyanine also ring-closes upon 267 nm excitation.

**Ultrafast Ring Closure.** In order to prove that 6,8-dinitro-BIPS can be photochemically switched on an ultrafast time scale, we will first concentrate on the ring-closure direction. Transient absorption with VIS pump pulses will demonstrate that the ring-closed product is formed on a picosecond time scale after merocyanine excitation. The reasoning is structured in two parts. First we will prove that merocyanine is photobleached by probing in the VIS region. Then we will show that the ring-closed product is formed by probing in the MIR.

**a. Visible Probing.** After photoexcitation of 6,8-dinitro-BIPS with a laser pulse centered at 560 nm, we observe the temporal and spectral behavior depicted in Figures 3 and 4. The spectral distribution consists of a strong bleach centered at 560 nm, excited-state absorption around 450 nm, and stimulated emission above 590 nm. This is similar to the behavior measured after 400 nm excitation of 1'-(2-carboxyethyl)-6,8-dinitro-BIPS.<sup>12</sup> The overall kinetics after 20 ps are best described by a sum of two exponentials and an offset, where the same fast time constant ( $\tau_{\text{fast}} = 98 \pm 3$  ps) and slow time constant ( $\tau_{\text{slow}} = 830 \pm 120$  ps) are used for all wavelengths (see resulting fit in Figure 4). The dynamics during the first 20 ps are partly ascribed to vibrational cooling<sup>11</sup> and therefore are ignored in the global fit routine.

After a pump–probe delay of 3.4 ns, the ultrafast dynamics are essentially over. It can be seen that the remaining bleach after 3.4 ns is very similar to the merocyanine absorption band in Figure 1. Direct comparison of the bleach at 3.4 ns and the

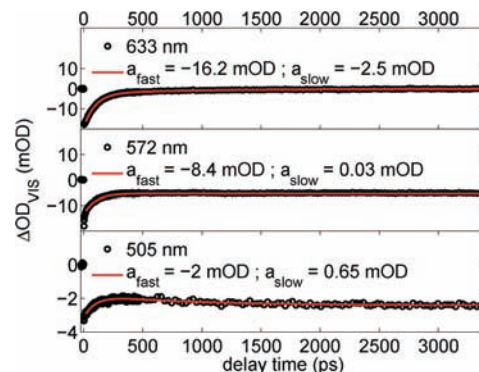


**Figure 4.** Single transients from Figure 3 at 633, 572, and 502 nm (top to bottom). A global fit routine (red lines), obtained by fitting each individual transient with two global time constants, results in  $\tau_{\text{fast}} = 98 \pm 3$  ps and  $\tau_{\text{slow}} = 830 \pm 120$  ps and the respective amplitudes  $a_{\text{fast}}$  and  $a_{\text{slow}}$  for each wavelength.

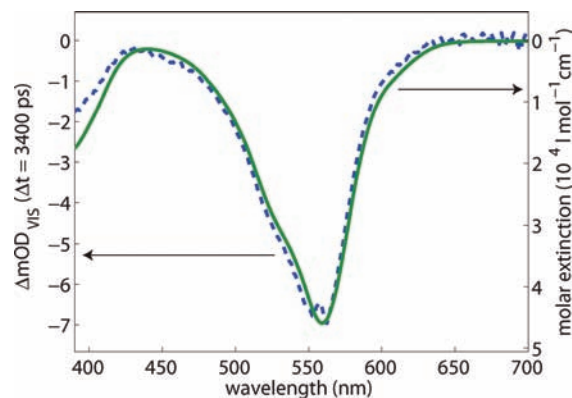


**Figure 5.** Merocyanine steady-state spectrum (green) in comparison with the difference spectrum (blue dashed) after 3.4 ns of the ring-closure experiments in the visible. The overall shape is quite similar. Thus the bleach can be assigned to reacted merocyanine. The small differences at the edges of the absorption band can be explained by changes in the distribution of at least two merocyanine isomers in the solution.<sup>37</sup>

merocyanine absorption in Figure 5 exhibits only small deviations at the band edges.

**b. Mid-Infrared Probing.** Since the produced spiropyran does not absorb in the VIS spectral region, the photobleach from our VIS probing experiments only indirectly suggests that spiropyran is formed. By contrast, we find direct evidence for the formation of spiropyran by analyzing the photoreaction in the MIR spectral region. For the structurally related 6-nitro-BIPS, it is known that ring closure shifts the symmetrical stretching mode of the nitro group to slightly higher frequencies and the absorption band becomes much stronger.<sup>38</sup> The top left panel of Figure 6 shows a difference FTIR spectrum after 2 min of illumination of the 6,8-dinitro-BIPS merocyanine with green continuous-wave (CW) light. The result is a similar shift and intensity change of the absorption as observed for 6-nitro-BIPS. Therefore, we used this absorption change and shift in the transient absorption of 6,8-dinitro-BIPS as direct spectroscopic indications of ring closure.

The transient absorption map for 6,8-dinitro-BIPS shown in the bottom left panel of Figure 6 was obtained after pumping with 400 nm light and probing between 1310 and 1360  $\text{cm}^{-1}$ .

(36) Würthner, F.; Archetti, G.; Schmidt, R.; Kuball, H. *Angew. Chem., Int. Ed.* **2008**, *47*, 4529–4532.

(37) Hobley, J.; Malatesta, V.; Millini, R.; Montanari, L.; Parker, W. O. N., Jr. *Phys. Chem. Chem. Phys.* **1999**, *1*, 3259–3267.

(38) Schiele, C.; Arnold, G. *Tetrahedron Lett.* **1967**, *8*, 1191–1195.

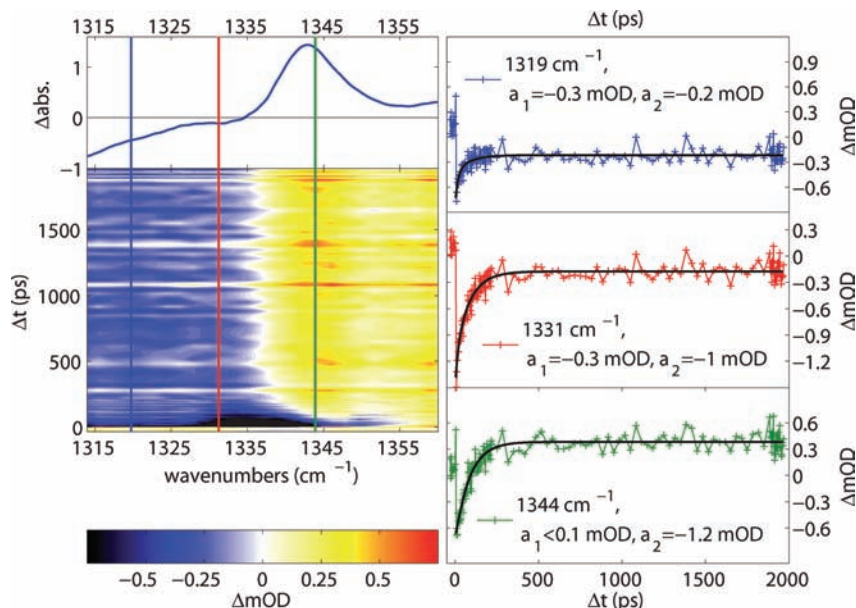


**Figure 6.** IR spectroscopy of 6,8-dinitro-BIPS. (Top left) FTIR difference spectrum after 2 min of irradiation of merocyanine with green CW light. Product absorption can be seen above  $1335\text{ cm}^{-1}$ , whereas reactant bleach can be seen below  $1335\text{ cm}^{-1}$ . (Bottom left) Transient absorption map of the same spectral region ( $\Delta\tilde{\nu} = 1.8\text{ cm}^{-1}$ ) with a pump wavelength of 400 nm, showing merocyanine bleach and recovery centered from  $1327$  to  $1346\text{ cm}^{-1}$  and the partially overlapping spiropyran formation at  $1344\text{ cm}^{-1}$  (from  $1336$  to  $1351\text{ cm}^{-1}$ ). (Right) Single transients of the left map (blue, red, green), with the transients obtained via the biexponential global fit routine in black ( $\tau_1 = 12 \pm 10\text{ ps}$ ,  $\tau_2 = 86 \pm 5\text{ ps}$ ). All transients are dominated by the merocyanine ground-state bleach recovery ( $\tau = 98\text{ ps}$  in the VIS, see Figure 4, and  $\tau = 86\text{ ps}$  in the MIR, deviations due to product formation). Spiropyran formation is proven in agreement with the FTIR spectrum by the remaining positive absorption at  $1344\text{ cm}^{-1}$ .

The main features of the map are a merocyanine bleach (from  $1327$  to  $1346\text{ cm}^{-1}$ ) and an additional slightly blue-shifted absorption band centered at  $1344\text{ cm}^{-1}$  (band from  $1336$  to  $1351\text{ cm}^{-1}$ ) that can be attributed to spiropyran formation due to the similarities of the dynamics to those of the structurally related 6-nitro-BIPS and the FTIR difference spectrum. We also performed this experiment with pump pulses centered at  $560\text{ nm}$ , resulting in the same characteristics.

All dynamics seen in the transient map decay during the first  $500\text{ ps}$ . A global fit routine with two exponential decays and an offset, taking into account only data points for times greater than  $2\text{ ps}$ , results in time constants of  $\tau_1 = 12 \pm 10\text{ ps}$  and  $\tau_2 = 86 \pm 5\text{ ps}$ . The time constant of  $98\text{ ps}$  for the merocyanine ground-state bleach recovery that was measured in the VIS spectral range is in close agreement with the time constant of  $86\text{ ps}$  obtained from these measurements in the MIR. We attribute the second time constant of  $12\text{ ps}$  to vibrational cooling of either the merocyanine or spiropyran ground state.<sup>11</sup>

The spiropyran formation, on the other hand, can be seen in the individual transients displayed in the three panels on the right side of Figure 6. The obtained global fit transients are shown in black to prove that all transients behave very similar. As mentioned above, they all start with a negative absorption change due to missing merocyanine ground-state absorption. The dynamics thereafter are dominated by the corresponding merocyanine ground-state bleach recovery, with only small deviations at early times due to vibrational cooling. Nevertheless, they differ in the remaining absorption change for delays  $>500\text{ ps}$ . The product formation is best seen in this remaining absorption: the absorption change at  $1344\text{ cm}^{-1}$  is initially negative, owing to the bleach, and becomes positive after  $100\text{ ps}$ , due to the product formation. If there were no absorption of the product at this position, a negative absorption change would remain here, too, as seen in the transients at  $1319$  and  $1331\text{ cm}^{-1}$ . Since absorption due to spiropyran formation is

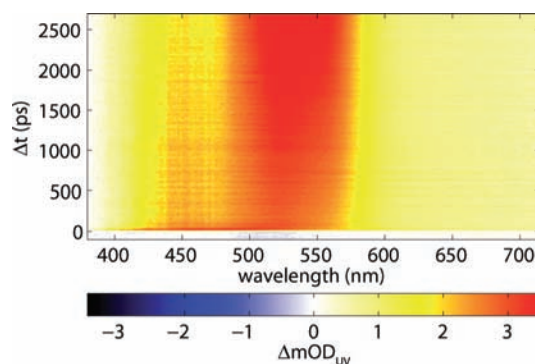


**Figure 7.** Transient absorption spectrum of the ring opening with  $267\text{ nm}$  pump and visible probe. After excitation, a positive absorption band emerges at  $450\text{ nm}$  and decays with increasing time. Around  $550\text{ nm}$ , different absorption bands associated with merocyanine structures increase with time.

overlaid with the bleach recovery and the characteristic decay changes from  $98$  to  $86\text{ ps}$ , we conclude that spiropyran formation is faster than merocyanine ground-state bleach recovery.

**Ring Opening.** Having shown that the ring closure is an ultrafast reaction, we now concentrate on the other switching direction, the ring opening. In these experiments the spiropyran isomer is created by illumination of the reservoir with green LEDs. Figure 7 shows the VIS transient absorption after excitation with  $267\text{ nm}$  laser pulses. Nonlinear optical processes and two-photon absorption in the solvent strongly contribute to the dynamics during the first picosecond after excitation. This prevents a simple analysis of data from these early times. After the decay of the initial dynamics, a broad transient absorption band covering the whole VIS spectral range from  $400$  to  $700\text{ nm}$  ( $\lambda_{\text{max}} = 500\text{ nm}$ ) (Figure 7) is apparent. The difference spectra at  $500$  and  $2600\text{ ps}$  (see Figure 8a) reveal that the absorption evolves into a spectrum with distinguishable shoulders at  $445$ ,  $525$ , and  $560\text{ nm}$  (black arrows) and a flat positive

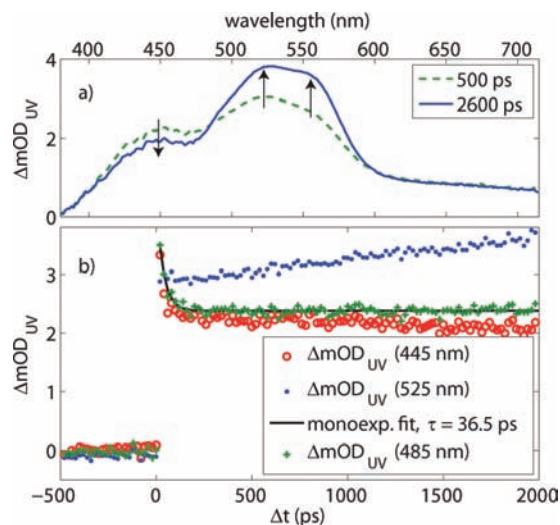


**Figure 8.** (a) Difference spectra of the ring opening at 500 and 2600 ps after excitation of the spiropyran form with 267 nm pulses. The development of the shoulders at 445, 525, and 560 nm is indicated by the black arrows. Further, an isosbestic point is identified at 485 nm. (b) Transients at two (445 nm, red open circles; 525 nm, blue dots) of the three shoulders of the absorption band of Figure 7 and at the isosbestic point (green crosses) and a monoexponential fit ( $\tau = 36$  ps, black).

offset above 620 nm. While the absorption decreases at 445 nm, it increases at 525 and 560 nm. An isosbestic point can be found at 485 nm. It should be noted that the shape and wavelength do not match the steady-state merocyanine absorption band in Figure 1 completely. For a more quantitative analysis of the dynamics, the transient absorptions at different wavelengths are plotted in Figure 8b. The data after 500 ps show increasing absorption at 525 nm (blue dots) and decreasing absorption at 445 nm (red circles). In contrast, the isosbestic point at 485 nm (green crosses) shows no dynamics after an initial fast decay. A fit of a single exponential and an offset to the data (black line) yields a time constant of 36 ps for this fast decay. The bidirectional switching results from the next section will help to interpret the dynamics found in the transient data of Figure 8. Hence, the interpretation is deferred to the end of the next section. There it will be shown that the broad VIS absorption band in Figures 7 and 8 is at least partly due to merocyanine in its electronic ground state.

**Ultrafast Switching.** Whereas ring-closed, unsubstituted BIPS can be opened to the ring-open ground state in a few tens of picoseconds,<sup>8</sup> it has been shown that the 6-nitro-BIPS is transferred into a long-lived merocyanine triplet state within a few picoseconds after excitation.<sup>13,26</sup> The question is therefore how the bisubstituted 6,8-dinitro-BIPS investigated in this work reacts and on what time scale it can be switched back and forth. Our approach to showing that the reaction product after excitation of the closed form, leading to the open form of 6,8-dinitro-BIPS, is generated in its ground state is re-excitation of the product. The experiments with direct excitation of the ring-open compound serve as a reference for the re-excitation experiments.<sup>7,39</sup> For this purpose, pump–repump–probe experiments were conducted as described in the Experimental Section.

**a. Bleach.** In Figure 9, we show the transient cooperative absorption signal  $\Delta\text{OD}_{2p}(560\text{ nm})$ , as defined in eq 1, averaged

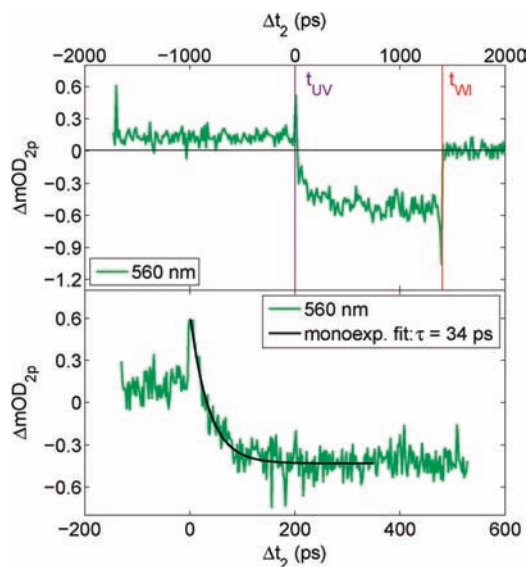


**Figure 9.** Transient absorption signal ( $\Delta\text{OD}_{2p}$ ) at 560 nm (averaged from 550 to 570 nm) due to the combination of the two pump pulses. The transient absorption can be divided into the three regions associated with the different pulse orderings explained in Figure 2 (A, closure–reopening; B, opening–reclosure; C, no pump–repump signal). (Top) Signal from  $-1.7$  to 2 ns. The positions of the UV pulse and the WL probe pulse are indicated by purple and red vertical lines, respectively. (Bottom) Measurement with higher temporal resolution for the transition from region A to region B. Here, the signal dynamics at the beginning of region B are emphasized. The black line corresponds to a monoexponential fit that results in a time constant of 34 ps.

over the wavelengths from 550 to 570 nm with respect to the delay time axis  $\Delta t_2$  in Figure 2. Note that the stronger noise compared to the two-pulse experiments from, e.g., Figure 3 is due to the fact that the cooperative three-pulse signal is 2 orders of magnitude lower ( $\sim 0.4$  mOD compared to  $\sim 20$  mOD). Nevertheless, the measurement technique described in the Experimental Section allows recovery of this transient with excellent sensitivity.

Zero signal in Figure 9 corresponds to a situation where the combination of both pump pulses yields the same result as the sum of the signals of the two individual pump–probe experiments (see eq 1). A positive value means that, due to the combination of the two pump pulses, a higher absorption is present at the time of the WL pulse. In the relaxed system (excluding reaction intermediates and thereby the dynamics seen in the bottom of Figure 9), such a positive value can only result from a higher spiropyran concentration at the time of the second pump pulse (which then induces more ring opening than in the individual experiment). Vice versa, a negative value can be explained by a spiropyran concentration decrease, e.g., a merocyanine concentration increase, at the time of the second pump pulse (which then induces more ring closure than in the individual experiment). Therefore, for an intuitive interpretation of Figure 9, one can say that the transient absorption corresponds to the change of the spiropyran concentration due to the first pulse at the time of the second pulse.

In region A, a small but nevertheless clearly positive absorption is visible, corresponding to a positive spiropyran concentration change. In this region of the time delay, the VIS pulse comes before the UV pulse. Since the used LED array does not completely close all merocyanine, the VIS pulse closes some of the small portion that is still present in the solution and thereby increases the spiropyran concentration by  $\sim 1/50$

(39) Larsen, D. S.; Papagiannakis, E.; van Stokkum, I. H. M.; Vengris, M.; Kennis, J. T. M.; van Grondelle, R. *Chem. Phys. Lett.* **2003**, *381*, 733–742.

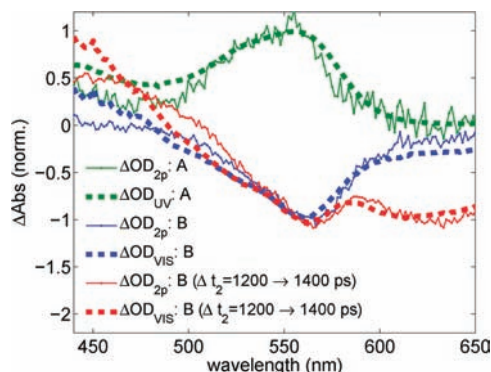


**Figure 10.** Comparison of the absorption change of the pump–repump combination ( $\Delta\text{OD}_{2p}$ , solid lines) to the absorption changes of the single-pump experiments ( $\Delta\text{OD}_{UV}$  and  $\Delta\text{OD}_{VIS}$ , dashed lines). The data are scaled for better comparison. To decrease the noise, the difference spectra were averaged over 20 delay positions. The signals  $\Delta\text{OD}_{2p}$  and  $\Delta\text{OD}_{UV}$ , averaged over the first nanosecond of region A, are shown in green. Spectra  $\Delta\text{OD}_{2p}$  and  $\Delta\text{OD}_{VIS}$  of region B are averaged from 400 to 900 ps and shown in blue. The red curves represent the signals  $\Delta\text{OD}_{2p}$  and  $\Delta\text{OD}_{VIS}$  at later times of region B (delay times from 1200 to 1400 ps).

( $\Delta\text{OD}_{UV} \approx 5$  mOD,  $\Delta\text{OD}_{2p} \approx 0.1$  mOD). The dynamics of the absorption change at 560 nm due to this ring closure are the same as those recorded in the two-pulse experiment ( $\Delta\text{OD}_{VIS}$ , see Figure 3). Therefore, these dynamics are canceled in the cooperative signal  $\Delta\text{OD}_{2p}$ . However, the following UV pulse acts on an increased spiropyran concentration ( $\sim 1/50$  higher), resulting in a slightly higher merocyanine production than recorded by  $\Delta\text{OD}_{UV}$  and a small positive offset remains when probing the effects of both pump and repump pulses.

Changing the pulse sequence to the delay region B (UV pulse before VIS pulse), the UV pulse mostly excites the spiropyran, since on the one hand the equilibrium is almost completely shifted to this form and on the other hand at 267 nm the extinction coefficient of the spiropyran is 2.5 times higher than that of the merocyanine. Again, the absorption change due to this process is not visible in  $\Delta\text{OD}_{2p}$  since it is the same as in  $\Delta\text{OD}_{UV}$ . However, the following VIS pulse acts on a higher merocyanine concentration and therefore bleaches more of the merocyanine compared to  $\Delta\text{OD}_{VIS}$ . This explains the negative absorption change in delay region B of Figure 9.

When the VIS pump reaches the sample after the probe pulse (delay region C), the signal  $\Delta\text{OD}_{2p}$  is equal to zero and only exhibits some noise, because the absorption change  $\Delta\text{OD}_{UV+VIS}$  is the same as  $\Delta\text{OD}_{UV}$ , whereas  $\Delta\text{OD}_{VIS}$  is zero.

We conclude that the signal in Figure 9 is due to ultrafast bidirectional switching.

**b. Spectral Shape.** Additional measurements for the spectral shapes of the absorption changes in the delay regions A and B are shown in Figure 10 to provide further proof for bidirectional switching. One has to consider that different isomers/conformers with different spectral shapes account for small deviations in the following comparisons, because the conformeric distribution after excitation is most certainly different from that in thermal equilibrium.

The thin green line represents the difference spectrum  $\Delta\text{OD}_{2p}$  of region A (averaged from  $-1700$  to  $-700$  ps). The dashed green line represents the difference spectrum recorded with the UV pump only ( $\Delta\text{OD}_{UV}$ ). Following the arguments given above, the two transient spectra should be very similar, because the UV pulse acts on a slightly increased concentration of the spiropyran. This is indeed reflected by the comparison of the two green lines in Figure 10.

The blue curves in Figure 10 are taken from the delay region B (averaged from 400 to 900 ps). In region B the spectral shape of  $\Delta\text{OD}_{2p}$  (solid) is similar to the shape of  $\Delta\text{OD}_{VIS}$  (dashed). This confirms our previous assignment of the underlying processes.

The red curves were also taken from delay region B, however at greater delay times such that the VIS pump is close in time to the WL probe (averaged from 1200 to 1400 ps). The general features that can be identified in the cooperative three-pulse signal  $\Delta\text{OD}_{2p}$  (red solid line in Figure 10) correspond to the dynamics in the transient map for the two-pulse ring closure of merocyanine (Figure 3), and thus also the difference spectrum (red dashed line in Figure 10) agrees. These dynamics are excited-state absorption (400–500 nm), ground-state bleach (550–600 nm), and stimulated emission (600–650 nm).

**c. Speed.** The experiment with higher temporal resolution of the transition from region A to region B shown in the bottom of Figure 9 allows us to determine the speed of merocyanine as well as spiropyran formation.

**Ring-Opening: A→B.** Beginning with the ring-opening reaction, i.e., merocyanine formation, we look at the dynamics of the transition from region A to region B. Initially (at  $\Delta t_2 = 0$  in Figure 9), a sharp peak can be detected in the three-pulse transient. Within approximately the first 100 ps after this sharp peak, a decrease from positive to negative absorbance is recorded. Whereas in delay region A the first pulse (VIS) decreases merocyanine concentration, in delay region B the first pulse (UV) increases merocyanine concentration. Therefore, the negative slope of the absorption change is expected. The decrease toward negative absorption change does not start at  $\Delta\text{OD}_{2p} = 0$  for  $\Delta t_2 = 0$  because reaction intermediates or hot spiropyran are formed after excitation of the spiropyran. For comparison see Figure 7 during the first 100 ps from 420 to 570 nm and Figure 8b. These intermediates absorb the VIS pulse without being able to reclose afterward. This corresponds to an effective reduction of VIS pump power that applies only to  $\Delta\text{OD}_{UV+VIS}$  and not to  $\Delta\text{OD}_{VIS}$ . Since  $\Delta\text{OD}_{VIS}$  at 560 nm is negative, the subtraction of  $\Delta\text{OD}_{VIS}$  from  $\Delta\text{OD}_{UV+VIS}$  leads to a positive  $\Delta\text{OD}_{2p}$ . Note also that the transient signal from Figure 9 cannot be explained by a dominating remaining merocyanine triplet state. Such a merocyanine triplet state would have similar effects to the ones observed for times slightly greater than zero in Figure 9. Hence, the signal in delay region B would always be positive.

For the following interpretation, we assume that the transient absorption band from 420 to 570 nm during the first 100 ps mentioned above in Figure 7 is not due to hot spiropyran molecules but to reaction intermediates. This assumption is supported by the fact that the absorption band is not continuous from the VIS spectral range to the spiropyran absorption in the UV spectral range but rather subsides at 420 nm. The decay of these reaction intermediates and the population increase of the merocyanine ground state have the same time constant. Thus, we interpret the dynamics after  $\Delta t_2 = 0$  as the dynamics of formation of merocyanine in the ground state. A monoexponential fit, shown as a black line in the bottom panel of Figure 9 starting at the temporal overlap of the two pulses, results in a time constant of 34 ps for the merocyanine ground-state formation. These dynamics are in agreement with the time constant of 36 ps at 485 nm that was determined in Figure 8. Changing the polarization angle between the two pump pulses from  $90^\circ$  to  $0^\circ$  did not lead to a change in the observed time constant.

**Ring Closure: B→A.** An upper boundary for the ring closure, i.e., spiropyran formation, reaction time can be extracted from the transition from region B to A. In Figure 9, the signal is nearly constant ( $\sim 0.1$  mOD) up to  $\Delta t_2 = -6$  ps. When the pump pulses cross (crossing at  $\Delta t_2 = 0$  from left to right in Figure 9), the absorption changes abruptly. Spiropyran formation is therefore very fast considering the large conformational change. This very fast reaction, whose signal is also obscured by vibrational cooling, does not allow an identification of putative intermediate merocyanine conformers. Nevertheless, the high speed of the ring closure is in good agreement with the MIR transient absorption experiments (Figure 6), which disclosed that ring closure is faster than the bleach recovery.

## Discussion

**Ring Closure.** It is known that the investigated merocyanine does not aggregate except in aliphatic solvents due to the steric bulkiness of the 3,3'-dimethylmethylene unit of the electron-donating indoline heterocycle.<sup>37,40</sup> We therefore exclude the possibility that dimer aggregates could be responsible for any observed signal. The two time constants (98 and 830 ps) observed when pumping and probing in the VIS spectral region are caused by two merocyanine isomers that coexist in thermal equilibrium. The existence of two isomers in polar solvents has been shown by NMR investigations in different solvents.<sup>37</sup> These studies concluded that the two isomers involved are the TTC and TTT isomers. Merocyanine isomers are named after the trans–cis configuration of the methine bridge; see the labeling in Figure 1. Participation of triplet states is excluded because the photoreaction is too fast for a triplet pathway.<sup>12</sup> CASSCF simulations have shown that a pure singlet reaction pathway via two conical intersections exists for the ring closure.<sup>41</sup>

**a. Product Identification.** To prove that photochemical ring closure occurs on the picosecond time scale, we will now focus on the MIR probe data to support our identification of the product. Experiments on the structurally related, unsubstituted and 6-nitro-substituted spiropyran compounds were published by Fidler et al.<sup>8,11,13</sup> By probing the ring-opening reaction with MIR pulses, they found that the two spiropyran absorption bands which do not overlap with merocyanine absorption bands are centered at 1340 and 1610  $\text{cm}^{-1}$ . These frequencies are very close to the vibrational modes assigned to the nitro group in the 6-position. For the present molecule, 6,8-dinitro-BIPS in chloroform, we do not see an isolated band at 1610  $\text{cm}^{-1}$  in the ring-closure experiments. Instead we observe a strong ground-state bleach at this spectral position (data not shown). This is also confirmed by the FTIR data. A spiropyran absorption at 1344  $\text{cm}^{-1}$ , on the other hand, is present in our species and can be traced back to the same vibrational mode as the absorption at 1340  $\text{cm}^{-1}$  in 6-nitro-BIPS (see the steady-state experiments and calculations in the literature<sup>38,42</sup>). Although the absorption change at 1344  $\text{cm}^{-1}$  after 2 ns due to the product formation is very small (Figure 6, green transient), it is nevertheless clearly positive. The direct conclusion from this positive absorption is that spiropyran is formed on an ultrafast time scale after photoexcitation of the merocyanine form of 6,8-dinitro-BIPS.

**b. Quantum Efficiency.** The quantum efficiency of a photo-reaction,  $\Phi$ , can be calculated from the initial bleach,  $I_i$ , and the remaining bleach,  $I_e$ , of an absorption that is characteristic for the reactant:

$$\Phi = \frac{I_e}{I_i} \quad (2)$$

We can apply this equation here, although vibrational cooling and overlap with product bands might affect the results. Hence the formula provides an estimate. In the present case we find 46% quantum efficiency for ring closure from the transient at 1322  $\text{cm}^{-1}$  in Figure 6.

In the VIS spectral region, bleach recovery is also observed (Figure 3), but here isomerization processes might have an influence on the result of eq 2. According to Figure 4, the slow component is zero around 572 nm. If we assume that the bleach in this spectral region is not superimposed by an excited-state absorption, we obtain a quantum efficiency of 40% for isomerization and ring closure. Since we do not observe significant isomerization in the difference spectrum in Figure 5, the bleach is mostly due to ring closure. The quantum efficiency of 40% thus obtained from the experiments probing in the VIS spectral range is in agreement with the 46% obtained from the experiments with MIR probing.

**Ring Opening.** For a better understanding of the dynamics after UV excitation of ring-closed 6,8-dinitro-BIPS, we first briefly review the known processes for the most investigated similar spiropyran, 6-nitro-BIPS and unsubstituted BIPS. For 6-nitro-BIPS, it was found that the triplet reaction plays a crucial role and rivals a possible singlet route.<sup>43</sup> It has been proposed that, following  $S_1$  excitation of the closed form, a rather complex succession of reaction intermediates takes place on the microsecond and millisecond time scales.<sup>43</sup> At 435 nm a slowly subsiding transient absorption has been found, and at 580 nm a slowly increasing absorption has been found. These findings have been assigned to the intersystem crossing of the merocyanine triplet state to the merocyanine ground state. It has been found that, 500 fs after excitation of the spiropyran in tetrachlorethene, the triplet of a vibrationally hot merocyanine isomer is formed.<sup>14</sup> This hot triplet relaxes with a time constant of 17 ps to the vibrational ground state. The cooling process follows an isomerization to a second isomer in the triplet state. In contrast to 6-nitro-BIPS, no triplet pathway was found after photoexcitation of the unsubstituted BIPS. According to transient MIR absorption experiments, the ring-opening reaction of the unsubstituted BIPS occurs on a time scale of 28 ps.<sup>8</sup> In the gas phase it has been shown that, after excitation with 267 nm (in the chromene subunit), a cascade of three reactions for nitro-substituted BIPS occurs.<sup>44</sup> C–O bond breaking with 40 fs is followed by isomerization to a cis-configured merocyanine around the central methine bond with 250 fs. The last reaction step, with a time constant of 12 ps, was attributed to the cis–trans isomerization of the central methine bond. The authors did not find any evidence for the two reaction mechanisms (one triplet, one singlet) suggested by TD-DFT calculations.<sup>45</sup> They assumed a singlet process for all molecules on the basis of the observed relaxation times.

(40) Würthner, F.; Yao, S.; Debaerdemaeker, T.; Wortmann, R. *J. Am. Chem. Soc.* **2002**, *124*, 9431–9447.

(41) Gómez, I.; Reguero, M.; Robb, M. A. *J. Phys. Chem. A* **2006**, *110*, 3986–3991.

(42) Futami, Y.; Chin, M. L. S.; Kudoh, S.; Takayanagi, M.; Nakata, M. *Chem. Phys. Lett.* **2003**, *370*, 460–468.

(43) Lenoble, C.; Becker, R. S. *J. Phys. Chem.* **1986**, *90*, 62–65.

(44) Poisson, L.; Raffael, K. D.; Soep, B.; Mestdagh, J.; Buntinx, G. *J. Am. Chem. Soc.* **2006**, *128*, 3169–3178.

(45) Sheng, Y.; Leszczynski, J.; Garcia, A. A.; Rosario, R.; Gust, D.; Springer, J. *J. Phys. Chem. B* **2004**, *108*, 16233–16243.



We will now consider these summarized findings from the literature with respect to our current findings on 6,8-dinitro-BIPS. Analogous to the findings in the literature, we see a decreasing absorption at 450 nm and an increasing absorption centered at 550 nm (Figure 8). However, during the first nanosecond the band changes much faster than the triplet pathway that was observed in 6-nitro-BIPS.<sup>28</sup> The broad, constant background above 600 nm observed in Figure 7 might suggest the possibility of a triplet or solvated electron contribution,<sup>46,47</sup> yet in a spectral region and on a time scale which has no impact on the interpretation of the ring-opening and ring-closing dynamics. Hence, we can safely conclude that the observed sub-nanosecond dynamics in 6,8-dinitro-BIPS do not involve triplet states. A possible explanation for the observed dynamics in Figures 8 and 9 is the existence of isomers/conformers that differ in their absorption spectrum from the completely relaxed ground state. Rotation/isomerization around the double bonds in the methine bridge would be hindered by the partial double bond character and the solvent, explaining the observed increase of the lifetime of the conformers from the 12 ps observed in the gas phase (observed for nitro-substituted BIPS) to the 34 ps for 6,8-dinitro-BIPS in this work. We do not detect any stimulated emission or excited-state absorption in Figures 7 and 8, an indication that these processes happen in the electronic ground state.

A fraction of the ring-opened product molecules can be closed back to spiropyran. This conclusion is supported by the observation that both the dynamics and the spectral shape of the bleach (Figures 9 and 10) are very similar to the bleach that results from simple excitation of the open merocyanine form. Therefore, we conclude that there is a significant subensemble which does not react along a triplet route. The second nitro group has a strong effect on the relative ground-state energies of the merocyanine and spiropyran forms. In contrast to 6-nitro-BIPS, 6,8-dinitro-BIPS is negatively photochromic.<sup>2</sup> Therefore, the electronic states of 6,8-dinitro-BIPS cannot be directly compared to those of 6-nitro-BIPS, and one cannot assume that intersystem crossing in the molecule studied here is as efficient as that in 6-nitro-BIPS. The time constant of 34 ps for the ring opening is furthermore in good agreement with the ring-opening speed of the unsubstituted BIPS (28 ps<sup>14</sup>), for which it is known that ring opening does not proceed along a triplet pathway.

In conclusion, we ascribe the fast, broad absorption observed in Figure 7 mostly to the ground state of transient ring-open forms that are very hot and cannot be assigned to a certain isomer. Afterward only the most stable isomers are formed, and therefore the spectrum converges toward the steady-state absorption spectrum of merocyanine. During this process the absorption between 440 and 490 nm decreases, whereas the absorption between 490 and 600 nm increases (Figure 8).

**a. Quantum Efficiency.** The quantum efficiency for ring-opening can be calculated in a good approximation from the photostationary equilibrium,  $[Me]/[Sp]$ , obtained while illuminating with 267 nm light. For this purpose, 267 nm femtosecond laser pulses with a beam diameter of 3 mm were used, leading to a decrease in intensity by a factor of  $9 \times 10^{-6}$  compared to the transient absorption experiments presented in Figures 7–10, thereby excluding contributions of two-photon

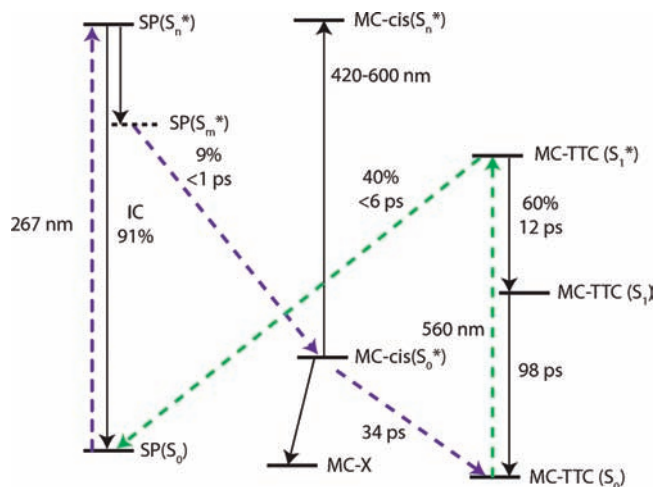


**Figure 11.** Investigated photoprocesses of 6,8-dinitro-BIPS. The ring-opening pathway is depicted by the purple dashed arrows. The ring-closure pathway is depicted by the green dashed arrows. \* represents a vibrationally excited state. “MC-cis” represents the reaction intermediates mentioned in the interpretation of the ultrafast switching section; “MC-X” represents unknown isomers and pathways that MC-cis relaxes to, as indicated by the UV-pump-only experiments. These isomers are converted thermally on a much longer time scale toward the MC-TTC isomer.

processes. Contributions of thermal ring closure and ring opening are neglected in this approximation since those reactions proceed on a time scale of minutes. Therefore, the extinction coefficients at 267 nm of both forms and the quantum efficiencies for ring opening and ring closure determine the equilibrium. The quantum efficiencies for ring closure of the merocyanine excited to the  $S_1$  ( $\Phi_{RC560}$ ) and  $S_2$  ( $\Phi_{RC400}$ )<sup>12</sup> states seem to be very similar (40%). Hence, we assume a similar quantum efficiency for 267 nm excitation ( $\Phi_{RC267} = \Phi_{RC560} = 40\%$ ). In this case we can roughly calculate the quantum efficiency for ring opening after complete relaxation ( $\Phi_{RO267}$ ) with

$$\frac{[Me]}{[Sp]} = \frac{\Phi_{RO267} \epsilon_{Sp267}}{\Phi_{RC} \epsilon_{Me267}} \quad (3)$$

where  $[Me]/[Sp]$  is the ratio of equilibrium concentrations. The extinction coefficients  $\epsilon_{Me267} = 14\,000 \text{ dm}^3 \text{ mol}^{-1} \text{ cm}^{-1}$  and  $\epsilon_{Sp267} = 32\,900 \text{ dm}^3 \text{ mol}^{-1} \text{ cm}^{-1}$  can be determined from Figure 1, and the quantum efficiency for ring closure,  $\Phi_{RC}$ , is known from the previous section.

The photostationary equilibrium while irradiating with 267 nm femtosecond laser pulses lies at approximately 50% of the initial merocyanine concentration, and therefore we determine  $\Phi_{RO267} \approx 9\%$ .

## Summary

By performing three-color pump–repump–probe experiments in the visible range, we have shown that a spiropyran-based molecular switch (6,8-dinitro-BIPS) can be switched photochemically in both directions on a picosecond time scale. We have furthermore reported the first direct observation of ring closure of a spiropyran on the picosecond time scale. Figure 11 summarizes our findings on the photochemistry of 6,8-dinitro-BIPS.

After ring opening of spiropyran with 267 nm femtosecond laser pulses  $[SP(S_0) \rightarrow MC\text{-cis}(S_0^*)]$ , transient absorption experiments probing in the visible spectral range reveal a mixture of isomers. The at least partial relaxation within 34 ps to the

(46) Kloepfer, J. A.; Vilchiz, V. H.; Lenchenkov, V. A.; Germaine, A. C.; Bradforth, S. E. *J. Chem. Phys.* **2000**, *113*, 6288.

(47) Vogt, G.; Nuernberger, P.; Gerber, G.; Improtà, R.; Santoro, F. *J. Chem. Phys.* **2006**, *125*, 044513.

merocyanine ground state MC-TTC( $S_0$ ) (purple dashed arrows in Figure 11) was shown by three-color pump–repump–probe experiments. The transient absorption experiments show that pathways to other merocyanine isomers exist. The resulting isomers of these pathways are denoted as “MC-X” since we cannot identify them any further. The overall quantum efficiency for ring opening obtained via the photostationary equilibrium is approximately 9%.

From three-color pump–repump–probe experiments we conclude that ring closure of the generated merocyanine ground-state species MC-TTC( $S_0$ ) can be induced with 560 nm laser pulses (dashed green arrows in 11). Transient absorption in the visible and mid-infrared spectral range provide proof for identification of the ring-closed product. Furthermore, these experiments show that the quantum efficiency for the ring-closure reaction is 40%. The ring closure to the spiropyran ground state completes the photocycle, as shown by the dashed lines in Figure 11. The high speed of the ring-closure reaction

( $\leq 6$  ps) suggests that the reaction starts from the vibrationally excited MC-TTC( $S_1^*$ ) state, because we see indications of vibrational cooling to the MC-TTC( $S_1$ ) taking up to 12 ps (Figure 6). The other 60% of the excited merocyanine molecules return to the merocyanine ground state with a time constant of 98 ps either via internal conversion or via fluorescence.

The results demonstrate that 6,8-dinitro-BIPS is a bidirectional molecular switch that can be switched back and forth on a picosecond time scale. Whereas common molecular switches have a high quantum yield for one of the two switching directions, the other direction is often much less efficient (Table 1). For the investigated system, however, the quantum efficiency is high for both directions. Thus, the molecule possesses a high potential for a multitude of applications.

**Acknowledgment.** J.B. acknowledges financial support from the “Fonds der chemischen Industrie”.

JA1062746